Detection of Object Anomalies Based on Intensity Distribution at Various Measurement Positions in Diffuse Optical Tomography System

Journal of Physics: Conference Series

Table of contents

Volume 1120

2018

Previous issue Next issue

The 8th International Conference on Theoretical and Applied Physics
20–21 September 2018, Medan, Indonesia

View all abstracts

Accepted papers received: 29 October 2018
Published online: 23 December 2018

Preface

IOP Conference Series: Materials Science and Engineering

Country	United Kingdom
Subject Area and Category	Engineering Engineering (miscellaneous) Materials Science Materials Science (miscellaneous)
Publisher	
Publication type	Conferences and Proceedings
ISSN	17578981
Coverage	2009-ongoing

13

H Index

SJR

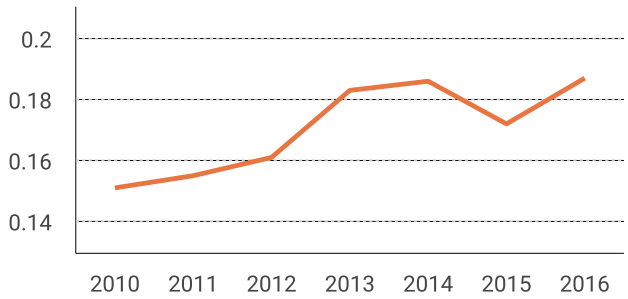

Citations per document

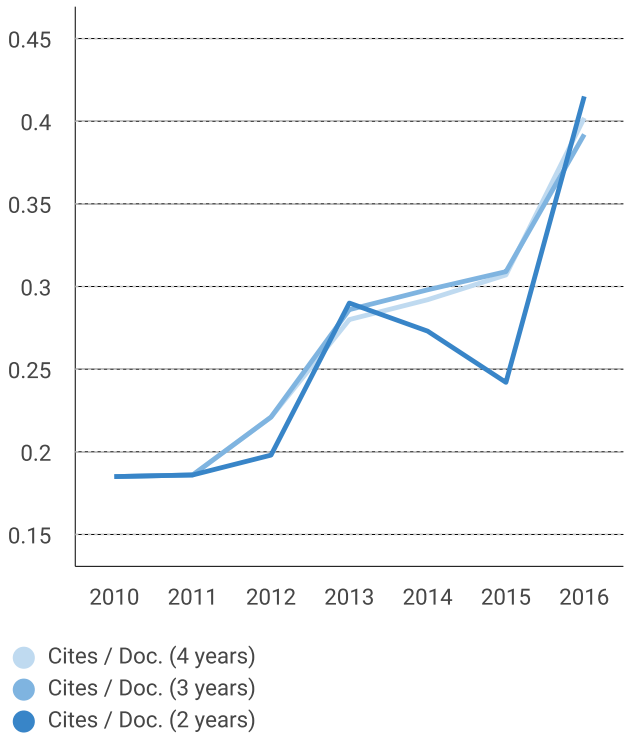

Total Cites Self-Cites

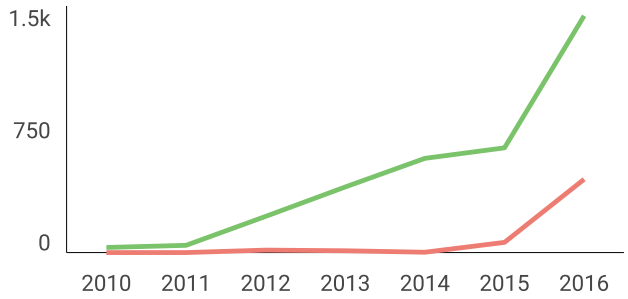

External Cites per Doc Cites per Doc

% International Collaboration

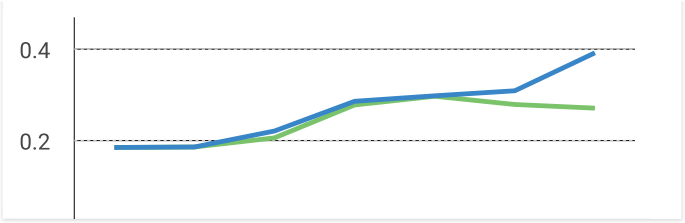

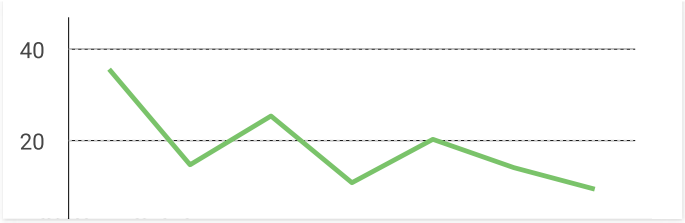

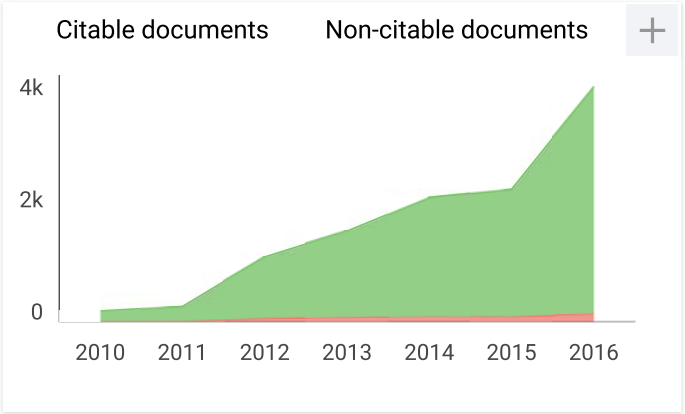

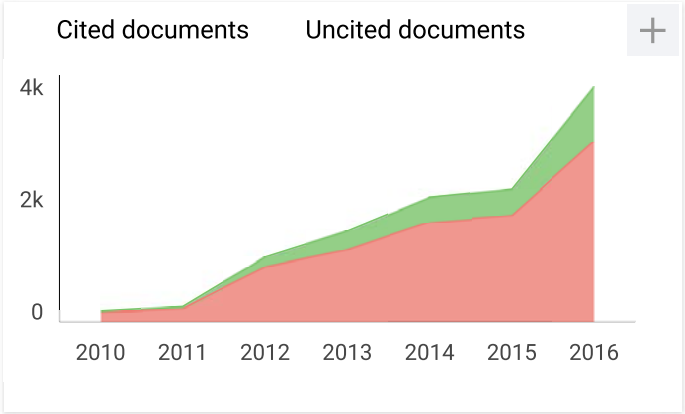

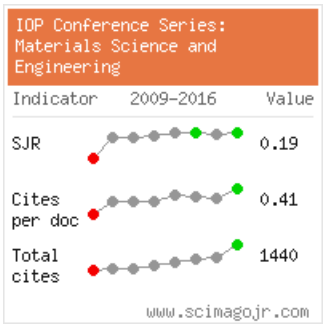

← Show this widget in your own website

Just copy the code below and paste within your html code:

<a href="http://www.scimag

Developed by:

Powered by:

Follow us on Twitter

EST MODUS IN REBUS
Horatio (Satire 1,1,106)

Detection of Object Anomalies Based on Intensity Distribution at Various Measurement Positions in Diffuse Optical Tomography System

N.Ukhrowiyah[a*], K.Ain[a], Samian[a], Y. G. Y. Yhuwana[a], and D.Prabaswara W[a]

[a]Department of Physics, Faculty of Science and Technology, Airlangga University, Surabaya 60115, Indonesia

*Corresponding Author's Email: nurilukhrowiyah@fst.unair.ac.id

Abstract. The determination of an object anomaly based on intensity distribution patterns in various measurement positions is proposed and investigated. This research was carried out in a simulation environment using numerical objects. They are a circle which consist of 248 elements. These objects include homogeneous and anomaly objects. The homogeneous object is made with the same values of absorption and scattering coefficients for all elements. Whereas, the anomaly object is made by adding different values of absorption coefficient and scattering on certain elements in homogeneous object. Both objects are illuminated by laser light from 16 different source positions. The intensity of light after passing objects is detected at 16 different positions as well. The intensity data passes through objects obtained by simulation based on the forward problem equation for continuous wave diffuse optical tomography (CW DOT) systems. The intensity different from the anomaly and the homogeneous object is plotted for each measurement position. The result showed that the characteristics of object anomalies (number, position and size) can be detected from the intensity distribution pattern at various measurement positions, respectively based on the number, position and the FWHM value of peak.

1. Introduction.

In recent years, optical-sources based tomography has been considerably developed which is called diffuse optical tomography, DOT [1]. The DOT technique is a technique of non-invasive, non-ionizing and relatively cheaper. This technique is widely used for the detection of breast cancer [2, 3, 4, 5], brain activity [6, 7], and small animal imaging [8]. The DOT technique is one of the promising imaging modalities that provide the spatial distribution of optical properties (absorption coefficient, scattering coefficients, and refractive index) within the object. In this technique, near infra red (NIR) light with wavelength range of 650-900 nm, is illuminated on the diffuse material. The spatial distribution of optical properties is mapped from measurements at the boundary of the material with a large number of pairs of sources and detectors.

The data measurements at the boundary of the material are the light intensity. Its distribution on the surface is captured by the detector. In general, the DOT system that is used to obtain the data at the boundary can be divided into three different categories: steady-state domain (SSD) or continuous wave domain method (CW) [9, 10, 11], frequency domain method (FD) [12,13,14], and time resolved domain method [15,16,17]. The time resolved and frequency domain methods exhibit high temporal resolutions (in the picosecond range for the time resolved and nanosecond for the frequency domain), but they have the disadvantages of high cost and complexity in the equipment [2,15]. In the SSD (CW) system, the light source continuously emits light onto the object and the amplitude of the outgoing light from the

boundary is measured. The continuous intensity system has the advantage of low cost and high dynamic range, as well as a relatively high signal to noise ratio (SNR) [2,15].

The intensity data measured from the CWDOT system is reconstructed by a specific reconstruction method to produce an image. Base on its image, an anomaly of object can be known. Pan, et al, [16], have shown that there is an intensity position deviation between heterogeneous phantoms (presence of anomalies) to the homogeneous phantom which is related to the angular orientation between anomalies and sources. Pandian and Singh [17], found that objects with anomalies at different depths had different peak intensities and different sizes of anomalies had different widths at half maximum (FWHM).

Based on the description, in this research, it will develop the method to determine an object anomaly based on intensity distribution patterns in various measurement positions of pairs of sources and detectors. This development is carried out by analysed the FWHM and the intensity deviation position between the heterogeneous and the homogeneous object to the source and detector position with various anomalous positions and sizes. This intensity distribution characteristic is used to map the position and size of anomalies. The results of this mapping are used to correct the reconstruction image, which generally unable to provide a clear boundary between anomalies and non-anomalies.

2. Materials and Methods

This research is carried out in a simulation using numerical objects. They are a circle which are divided into 248 small triangular elements connected with 141 nodes. These objects include homogeneous and anomaly objects. The homogeneous object is made by giving the same values of absorption and scattering coefficients for all elements. Whereas the anomaly object is made by adding different values of absorption coefficient and scattering on certain elements in homogeneous object. Figure 1 is an example of a homogeneous numerical object, with one anomaly and two anomalies.

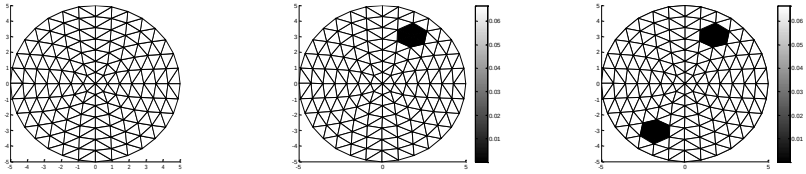

(a) (b) (c)

Figure 1. Numeric object a) Homogeneous; b) With 1 anomaly; c) With 2 anomalies

The objects are illuminated by laser light from 16 different source positions. The intensity of light after passing objects is detected at 16 different positions as well. The intensity data passes through objects obtained by simulation based on the forward problem equation for continuous wave diffuse optical tomography (CW DOT) systems.

In the CW case, the diffusion equation (DE) can be written as [18]

$$-D(r)\nabla\phi(r) + \mu_a(r)\phi(r) = q(r) \quad (1)$$

Where $\boldsymbol{r}$ is the location in the tissue domain Ω, $\Phi(\mathbf{r})$ is the photon density distribution, $\mu_a(\mathbf{r})$ is the absorption coefficient distribution, $q(\mathbf{r})$ is the source term, D is the diffusion coefficient given by $D = 1 / [3(\mu a + \mu_s^{'})]$, where$\mu_s^{'} = (1-g)\mu_s$ is the reduced scattering coefficient, μ_s is the scattering coefficient, and g is the anisotropic factor. The finite element method (FEM) is used to solve equation (1) and generate the model data $F(\mu_a)$ for a given distribution of the absorption coefficient.

The FEM Formulation of first equation (1) is

$$\lceil D(r) + C(\mu_a) + F \rceil \phi = Q \quad (2)$$

Where

$$K_{ij} = \int_\Omega D(r)\nabla b_i(r)\,\nabla b_j(r) d\Omega \quad (2a)$$

$$C_{ij} = \int_\Omega \mu_a(r) b_i(r)\, b_j(r) d\Omega \quad (2b)$$

$$F_{ij} = \frac{1}{2A}\int_{\partial\Omega} b_i(r)\,\nabla b_j(r) d(\partial\Omega) \quad (2c)$$

with $bi(r)$ and $bi(r)$ are linear basis function.

In this research, the model data $F(\mu_a)$ is used as simulated data intensity. The simulated intensity data different from the anomaly (I_{an}) and the homogeneous object (I_{an}) that is named as ΔI, with

$$\Delta I=(I_{hom}-I_{an}) \quad (3)$$

The value of ΔI is plotted for each measurement position source and detector. Based on this scheme of intensity distribution, an anomaly of object can be determined.

3. Result and Discussion

The numerical object is scanned by forward problem programs [19] so that the intensity data is obtained at all nodes. The intensity data at the node is used only on the object boundary. This is adjusted to the real conditions where data acquisition can only be done on the boundary of the object. The intensity data profiles as various measurement positions for objects with 1 anomaly and 2 anomalies that are compared to intensity data for homogeneous object are shown in Figures 2 and 3. The profile one projection intensity data (one source position with various detector positions) on a homogeneous object, with 1 anomaly, and 2 anomalies shown in Figure 4.

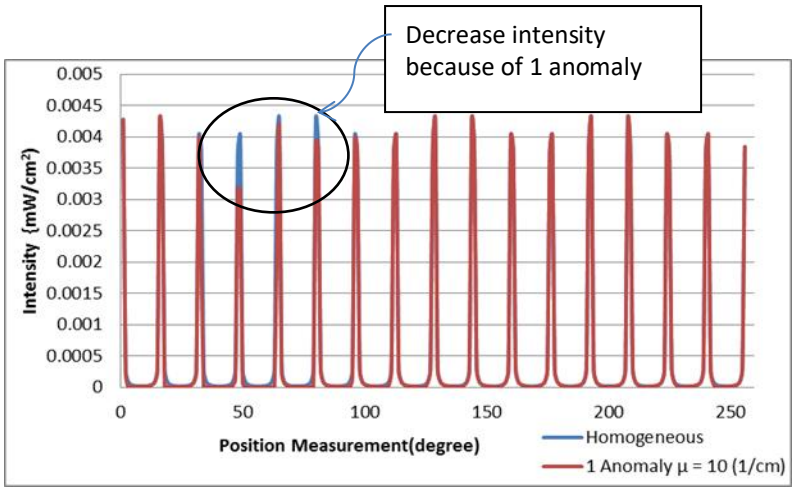

Figure 2. Comparison of intensity data profile of objects with 1 anomaly to homogeneous objects

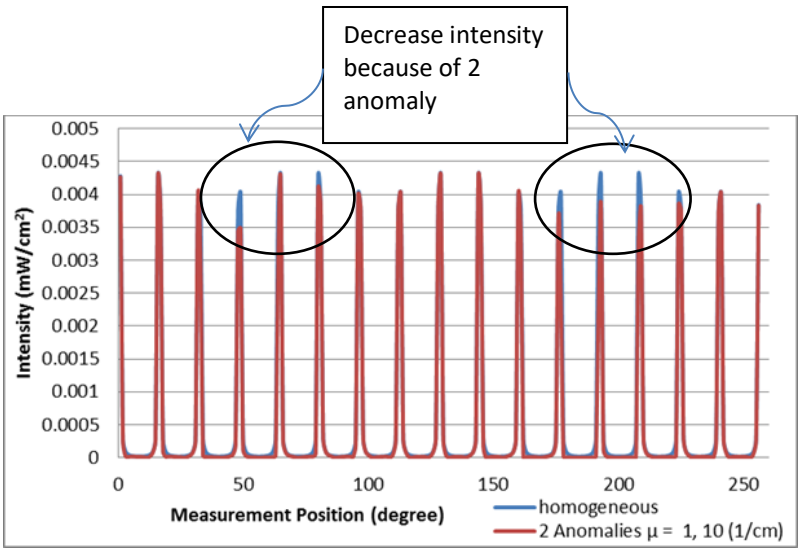

Figure 3. The comparison of intensity data profile of objects with 2 anomalies to homogeneous objects

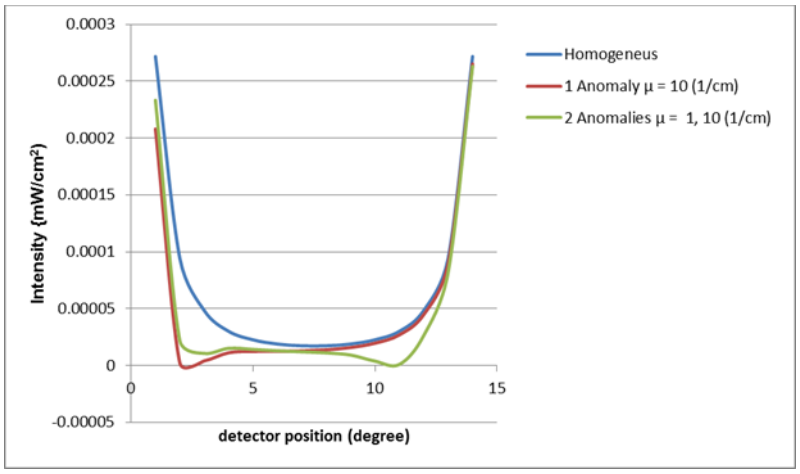

Figure 4. The intensity data profile of objects for a projection of homogeneous objects, objects with 1 and 2 anomalies

Based on Figure 2 and.3 which is the intensity data profile of objects with 1 and 2 anomalies compared to homogeneous objects, shows a decrease of intensity at certain positions as a result of an anomaly in the object. The figure 4 shows the intensity data profile of one projection for a homogeneous object, an object with 1 and 2 anomalies. It can be seen that for the homogeneous objects (without anomalies) having a certain profile pattern same as the U letter. Besides that, the object with anomaly has an indentation at the bottom when compared to the homogeneous object

The numerical object with anomaly and graph of distribution of ΔI values to the measurement position are shown in Figure 5. Based on Figure 5, it can be observed that the graph of the distribution of distribution ΔI values to the measurement position for objects with 1 anomaly (Figure 5B) has 1 peak whose position corresponds to the position of anomalies on numerical objects (Figure 5A). The same thing is shown for objects that have 4 anomalies, the graph of the distribution of ΔI values to the measurement position for objects with 4 anomalies (Figure 5D) has 4 peaks whose position corresponds to the anomaly position on numerical objects (Figure 5B). Thus, it can be said the number and position of an object anomaly qualitatively can be determined based on the number and position of the peak in the graph distribution of the value of ΔI to the measurement position

The minimum separation distance (resolution) between 2 peaks on the distribution of the ΔI value to the measurement position is searched by scanning numerical objects with 2 anomalies at various distances. The numerical objects with 2 anomalies which is the separation distance between anomalies is 2 elements and the graph of the distribution of ΔI values to the measurement position are shown in Figure 6. Based on Figure 6, it can be shown that objects with more than one anomaly can be seen if the distance between anomalies is 2 elements. This is showed by the graph of the distribution of the ΔI value to the measurement position (Figure 6B) that the peaks of the ΔI value are still visible with the distance between anomalies as 2 elements.

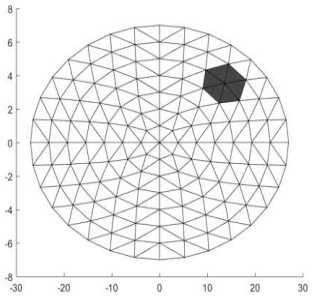

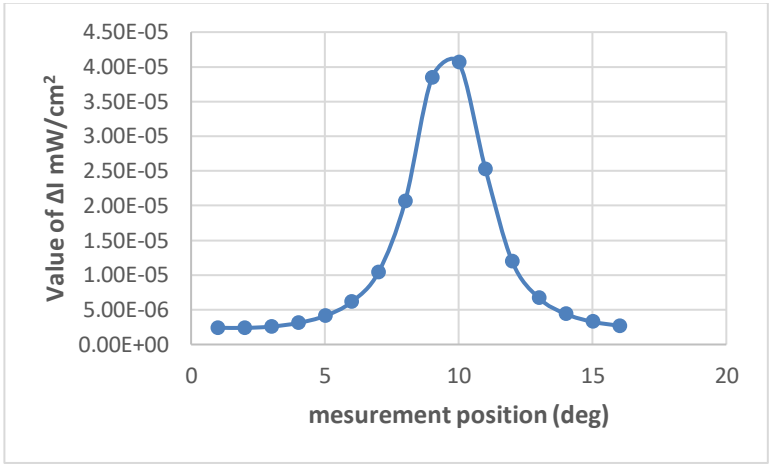

(a) (b)

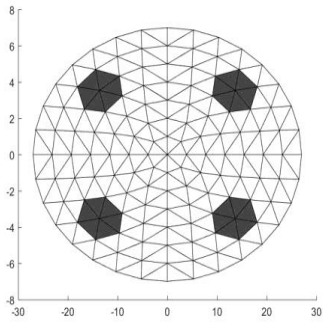

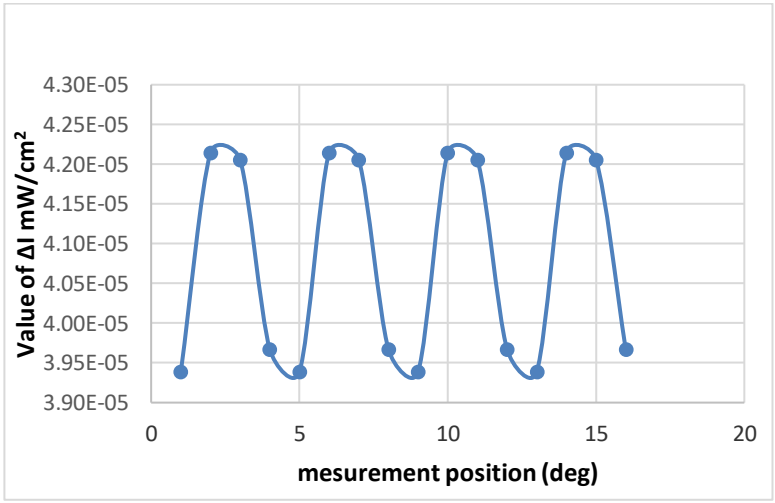

(c) (d)

Figure 5. Numeric object with (a) 1 anomaly (c) 2 Anomalies and distribution ΔI values to the measurement position for (b) 1 anomaly (d) 4 Anomalies

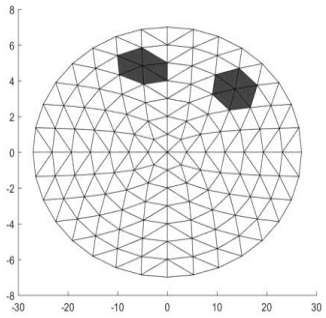

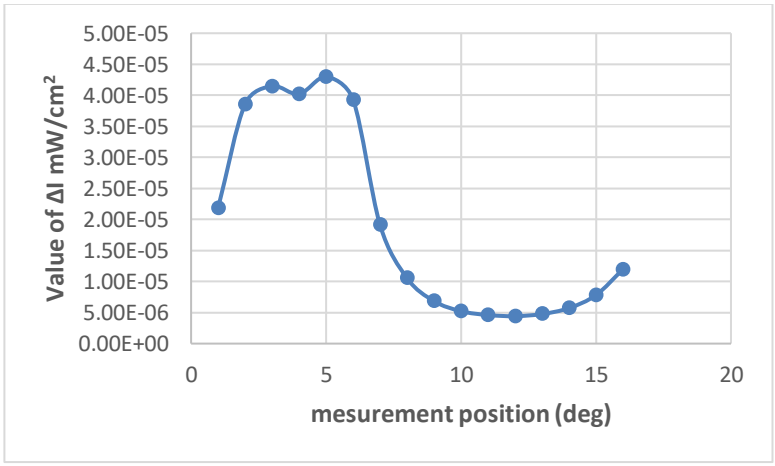

(a) (b)

Figure 6. The numeric object with 2 anomalies which the separation distance between anomalies is 2 elements and the graph of the distribution of ΔI values to the measurement position.

Table 1. The value of FWHM and peak ΔI object with 1 anomaly

Path (cm)	FWHM (cm)	Peak value ΔI (mW/cm^2)
7	1.053729	0.0000804
6	1.500141	0.0000483
5	2.314043	0.0000417
4	3.465781	0.0000371
3	5.30394	0.0000338
2	8.829681	0.0000308

The values of FWHM and ΔI peaks for objects with 1 anomaly at 1 element on various paths are shown in Table 1. The deepest part of the object is indicated by the smallest path, and the outer part of the object is indicated by the largest path. Based on Table 1, it can be shown that the deeper the anomaly position, the greater the FWHM value and the smaller the peak value.

Table 2. The value of FWHM and ΔI peak object with 1 anomaly in different sizes

Anomaly size (element)	FWHM (cm)	Peak value ΔI (mW/cm^2)
1	2.386	0.0000397
2	2.774	0.0000408
3	2.979	0.0000416
4	3.614	0.0000412

The values of FWHM and ΔI peaks for objects with 1 anomaly of different sizes on the same path are showed in Table 2. Based on Table 2, it can be shown that the greater the size of the anomaly the greater the FWH M value and the peak

4. Conclusion

In this research, the method to determine an object anomaly based on intensity distribution patterns in various measurement positions of pairs of sources and detectors is developed. The number and position of an object anomaly qualitatively can be determined based on the number and position of the peak on this distribution. The resolution between two peaks is two elements. The size of object anomaly can be determined based on the FWHM value. The deeper the anomaly position, the greater the FWHM value and the smaller the peak value. The greater the anomaly size, the greater the FWHM value and the peak.

5. Reference

[1] A.P. Gibson , J.C. Hebden and S.R. Arridge , 2005, Recent Advances in Diffuse Optical Imaging, Physics Medicine and Biology, 50, R1–R43
[2] M. Xiao, Y. Jiang, Q. Zhu, S. You, J. Li, H. Wang, X. Lai, J. Zhang, H. Liu, J. Zhang, 2015, Academic Radiology, 22(4), 439-446
[3] B. W. Pogue, Shudong J., Christine K., 2004, Journal of Biomedical Optics 9(3), 541–552.
[4] R. Choe, 2005, Diffuse Optical Tomography and Spectroscopy of Breast Cancer and Fetal Brain, *Dissertation*, Faculty Physics and Astronomy University Pennsylvania.
[5] Z. G. Wang , L.Z.Sun and L.L.Fajardo, 2009,Communications In Numerical Methods In Engineering, 25, 657–665
[6] F. Tian, and H. Liu, 2014, NeuroImage, 85(1), 166-180

[7] T. Austin, A.P. Gibson, G. Branco, R.Md. Yusof, S.R. Arridge, J.H. Meek, J.S. Wyatt, D.T. Delpy, and J.C. Hebden, 2006, NeuroImage ,31, 1426 – 1433.
[8] M. Bruno, P. Poulet, 2006, Nuclear Instruments and Methods in Physics Research *A* 569: 551–556.
[9] M. Pan, C. Chen, M. Pan and Y. Shyr, 2009, Measurement, 42, 377.
[10] H. Feng, J. Bai, X. Song, G. Hu, and J. Yao, 2007, International Journal of Biomedical Imaging, Article ID 28387, 9 pages
[11] M. A. Ansari and E Mohajerani, 2014, Physics Letters A, 378 (40), 2981-2984
[12] O. Balima, J.Boulanger, A.Charette, D.Marceau, 2011, Journal of Quantitative Spectroscopy & Radiative Transfer, 112,1229.
[13] Y. S. Jun and W. S. Baek, 2010,Journal of Physics: Conference Series 224,012146.
[14] N. Ducros, C. D'Andrea, A. Bassi, F. Peyrin, 2011, IRBM, 32(4) 243-250
[15] J. Wang., 2009, Broadband Near Infrared Tomography for Breast Cancer Imaging, Disertation, Departement of Physiscs and astronomy, Darmoth college, Hanover, New Hampshire.
[16] M. C. Pan, C.H. Chen , M.C. Pan and Yi-Ming Shyr, 2009, Calibration, and Performance, *Measurement 42* : 377–389
[17] P. S. Pandian and M. Singh, 2010, Indian Journal of Experimental Biology, 48, 993-1001
[18] R. P. K. Jagannath and P. K. Yalavarthy, Journal of Biomedical Optics, 17(10), 106015 (2012)
[19] N.Ukhrowiyah and M. Yasin, 2017, AIP Conf. Proc. 1888, 020038-1–020038-7, AIP Publishing